Pet. Sci. (2017) 14:648–661
DOI 10.1007/s12182-017-0197-7

ORIGINAL PAPER

# Late Cenozoic seismic stratigraphy of the Andaman Forearc Basin, Indian Ocean

**Dhananjai K. Pandey[1] · Goli Anitha[1] · Ramesh Prerna[1] · Anju Pandey[1]**

Received: 16 November 2016 / Published online: 7 November 2017


**Abstract** Interpretation of new multichannel seismic reflection data from the Andaman Forearc Basin (AFB) in the northern Indian Ocean is presented here. The high-quality multichannel seismic data from the Andaman Forearc region enable us to examine the seismic characters and to demarcate seismic sequences bounded by distinct unconformities. Ages of marked seismic horizons have been calibrated with available litholog data from nearby industry boreholes. Seismic interpretation of new data shows that the AFB is filled with ~ 4.5-s-two way travel time (TWT) thick Neogene to Recent sediments. The entire basin assemblage exhibits two distinct major sequences pertaining to the Neogene and Quaternary times. A large part of the basin is filled with intermittent mass transport deposits (MTD). We infer that the episodic uplift of the Invisible Bank, protuberance of the outerarc and regular deformation through reactivation of preexisting normal faults since the Pleistocene could be attributed as causal mechanisms for the MTDs. Strong bottom simulating reflectors are identified in the Late Miocene and younger sediments of the outerarc and AFB at a depth of ~ 0.6 s TWT and correspond to the presence of gas hydrates in this region. Our interpretations have significant implications for geodynamic as well as resource exploration in the AFB.

✉ Dhananjai K. Pandey
pandey@ncaor.gov.in; dhananjai@gmail.com

[1] ESSO-National Centre for Antarctic and Ocean Research, Headland Sada, Vasco da Gama, Goa 403 804, India

Edited by Jie Hao

**Keywords** Andaman Forearc Basin · Neogene · Uplift · Invisible Bank · Outerarc · Stratigraphy

## 1 Introduction

The convergence process of Indo-Australian plate with Southeast Asian plate (Eurasian) has been active since the Paleogene (Hall 2011, 2012). Consequently, the oceanic lithosphere has been subducting beneath the Southeast Asian plate along the Sunda arc extending up to the Himalayan syntaxis in the north in an almost arc-parallel direction (Fig. 1). The Andaman-Nicobar subduction zone is the northwestern limb of the Sumatra–Andaman subduction system. The convergence varies in terms of speed as well as direction from Sumatra in the south through the Andaman Islands in the north (Rao and Kumar 1999; Sieh and Natawidjaja 2000). GPS measurements show that the direction of movement of the Indian plate relative to the Sunda plate is to the NNE at a rate of *c.*43 mm/year (McCaffrey 1992; McCaffrey et al. 2000). The present trace of subduction lies at the western flank of the Andaman-Nicobar ridge (Fig. 1). A rather oblique convergence resulted in a strike-slip fault along the trench axis, formation of forearc and back-arc basins and seafloor spreading (Curray et al. 1979; Curray 2005). The tectonics of the Andaman-Nicobar region has been discussed in detail by several researchers (Rodolfo 1969; Curray et al. 1979; Kamesh Raju et al. 2004, 2007; Curray 2005; Singh et al. 2013; Moeremans et al. 2014; Singh and Moeremans 2017; and references therein).

The rate of plate convergence along the Eurasian margin has varied significantly over time (Katili 1973, 1975). It increased significantly after the northward drift of India in

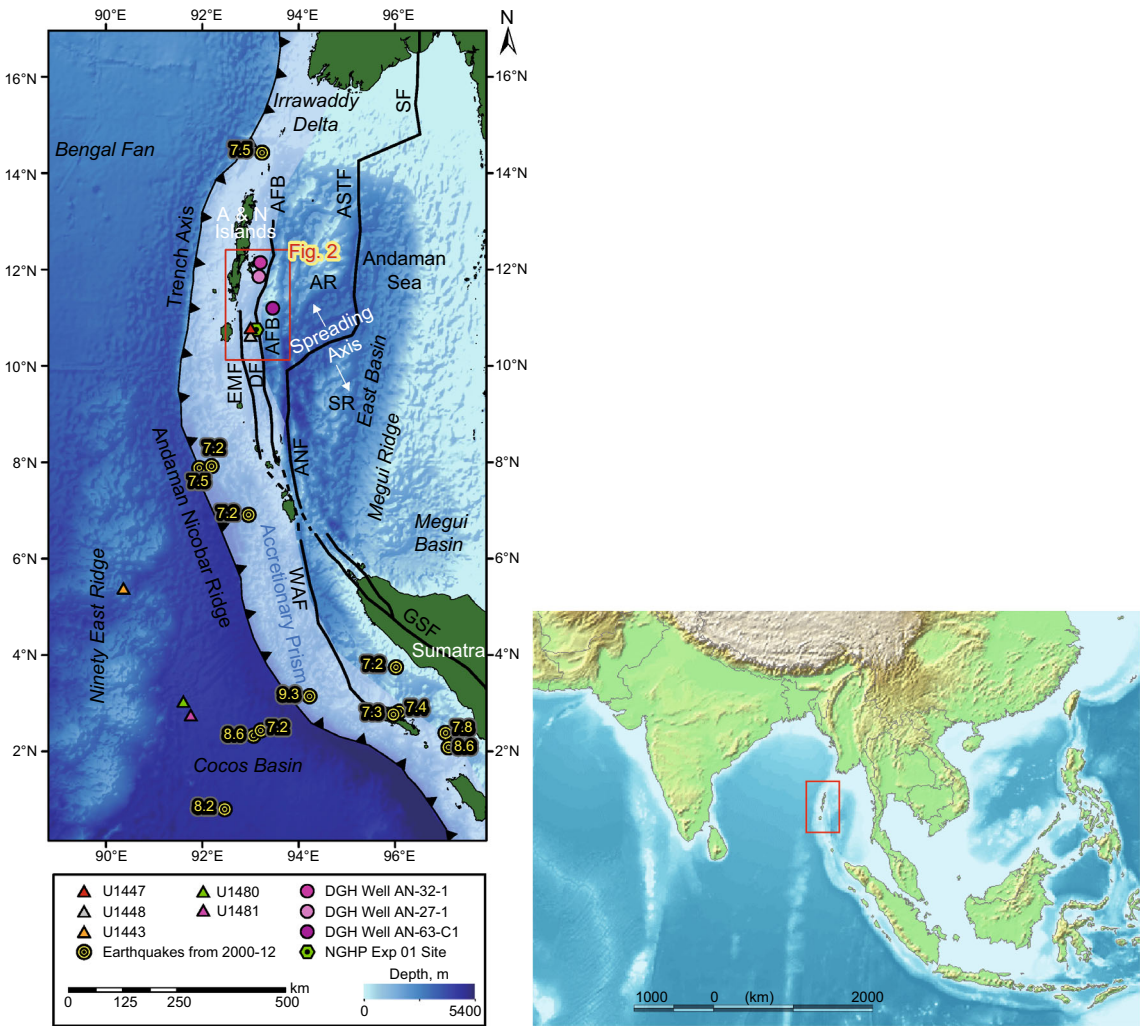


**Fig. 1** Regional map showing major geomorphic/tectonic features of the Andaman-Sumatra subduction system. The inset map shows the location of Andaman subduction zone in a regional context. The Andaman-Sumatra trench axis is shown by thick black line with solid triangles. Past earthquakes since 2000 having Mw > 7 are overlain on the map with their respective magnitudes. Recent IODP deep-sea drill sites are shown with respective site numbers. Various acronyms are: the East Margin Fault (EMF); Diligent Fault (DF); the Andaman Forearc Basin (AFB); Alcock rise (AR); and Sewell rise (SR) on the either side of the spreading axis. Traces of West Andaman Faults (WAF); Andaman-Nicobar Fault (ANF); the Andaman Sea Transform Fault (ASTF); Great Sumatra Fault (GSF); and Sagaing Fault (SF). Locations of various wells are shown on the map. The rectangular box shows the study area. See Fig. 2 for the seismic lines used in this study

the late Cretaceous. The extent of the subduction margin became about 6000 km long by the Cenozoic. The oblique collision of India with Eurasia at ~ 44 Ma culminated into arcuate compressional structures. These features are evident in strike-slip sliver faults such as the Sagaing Fault (Fig. 1) and the Western Andaman Fault (Peltzer and Tapponnier 1988; Curray 2005). The relocation of the volcanic arc from the Megui ridge (Fig. 1) further west finally led to the extension in the Megui Basin in the late Oligocene (Ghosal et al. 2012; Moeremans and Singh 2015). The entire Andaman Basin is ~ 1200 km long and extends from the Irrawaddy delta coast of Myanmar in the north to the Sunda trench in the south with a maximum E–W stretch of ~ 600 km (Fig. 1). The Irrawaddy delta sediments are the principal sedimentary source of the basin (Rodolfo 1969). The giant 2004 Andaman-Sumatra earthquake ruptured the greatest fault length of any recorded earthquake, spanning across more than 1200 km along this subduction system. The Andaman-Nicobar segment experienced the second-largest slip of the rupture area (c. 20 m; Gahalaut et al. 2010) and a significant near-trench slip (Moeremans et al. 2014; Singh et al. 2013). The major morpho-tectonic features observed in the Andaman Basin are the outerarc, AFB, Invisible Bank (IB), back-arc basin, volcanic arc and Alcock-Sewell seamount complexes, etc. (Fig. 1). In general, the sediment subsidence and uplift of

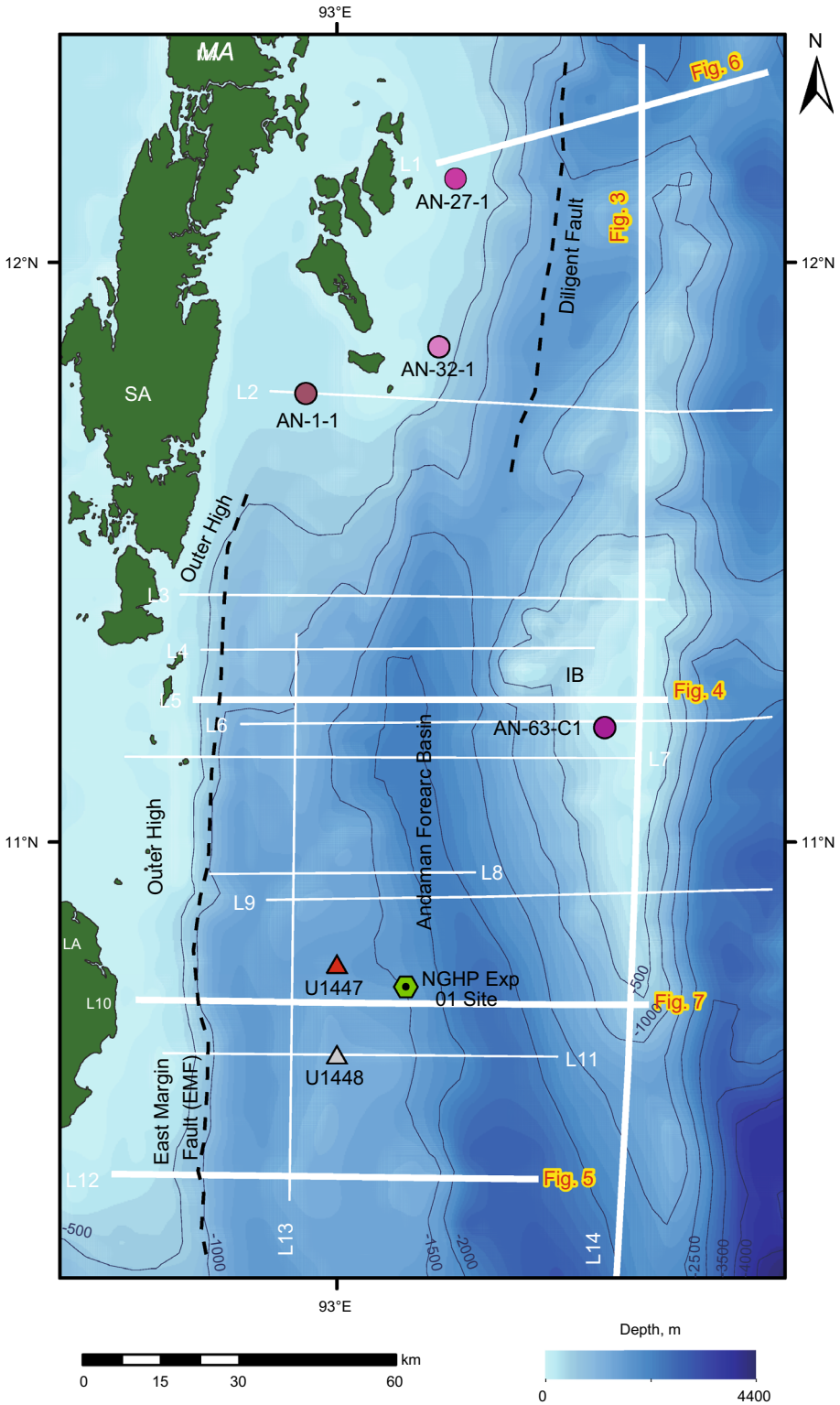


**Fig. 2** E–W and N–S extents of the seismic tracks (L1–L14) used in this study superposed on the satellite bathymetry map after Sandwell and Smith (2009). The thicker lines represent the seismic sections discussed here. Locations of various drill holes in the area are as in Fig. 1. Andaman-Nicobar islands (MA Middle Andaman and SA South Andaman, LA Little Andaman); outerarc ridge/high, Invisible Bank (IB)

the accretionary wedge is reported as the main influencing factor for the formation of the Forearc/Narcondam deep basin (depression) between the outerarc ridge and the volcanic arc (Moeremans et al. 2014). The Andaman-Nicobar ridge was formed during the Oligocene to Eocene time due to east–west compression of sediments of the Malayan shelf (Rodolfo 1969). This ridge mainly consists of ophiolites and scraped off sediments from the downgoing Indian plate and the Neogene shallow water sediments of the forearc environment (Curray et al. 1979; Curray 2005; Moeremans and Singh 2015).

The AFB has been formed because of the subduction process near the Andaman-Sumatra convergent boundary. It is one of the key geological units of the Andaman subduction zone as knowledge about the depositional systems in the forearc has the potential to elaborate a series of past tectonic events, directly associated with the subduction processes. Moreover, the Andaman Forearc has strong significance in terms of hydrocarbon potential proven by previous gas hydrate studies (Kumar et al. 2014). The marine gas hydrates developed in this area are found to be at greater depths compared to those in other parts of the world, and their presence is confirmed by recent drilling activity of NGHP (National Gas Hydrate Program of India) Expedition-01 (Kumar et al. 2014). The history of long-term sedimentation processes in the past also holds the key for understanding monsoon variability in South Asia. In order to explore the long-term links between the two, an International Ocean Discovery Program (IODP) expedition (IODP-353) carried out drilling and coring at sites U1447 and U1448 in this region (Fig. 2) during early 2015 (Clemens et al. 2015).

The stratigraphy and structural evaluation of the forearc off northern Sumatra to Java is fairly well documented (Beaudry and Moore 1985; Izart et al. 1994; Susilohadi et al. 2005; Mosher et al. 2008; Berglar et al. 2008, 2010; Moeremans et al. 2014; Singh and Moeremans 2017). In contrast, the seismic stratigraphy of the Andaman Forearc region and its structural details have not been precisely described so far, due to the lack of adequate high-quality depth-controlled data. Hence, there exists a requirement to document seismic stratigraphy of the Andaman Forearc using closely spaced high-quality 2D multichannel seismic (MCS) in both E–W and N–S directions, with a depth control of $\sim$ 7 s (TWT). Here, we concentrate on the depositional environments and associated structures within the regional stratigraphic framework of the AFB. Our seismic-lithological interpretation, in association with the new deep-sea drilling information from sites U1447 and U1448 (Fig. 2) of the IODP Expedition-353 (Clemens et al. 2015), would provide important insights into the understanding of sedimentary processes in the Andaman Forearc region.

## 2 Data and methodology

About 1000 km of MCS reflection data have been analysed for the present work (Fig. 2) from a total of more than 2500 km of seismic data acquired by the Directorate General of Hydrocarbons (DGH), India, during 2002–2003. The seismic data with a recording length of 8 s two-way travel time (TWT) along E–W and N–S profiles were processed up to the prestack time migration stage. In addition to the seismic data, satellite bathymetry data from Sandwell and Smith (2009) were taken into account to understand the detailed morphology and structures of the AFB. Besides these, distinct seismo-geological boundaries are constrained by available industry lithologs (such as AN-1-1: https://www.ndrdgh.gov.in/NDR/Images/AndamanBasin/andaman22.jpg and borehole AN-32-1 https://www.ndrdgh.gov.in/NDR/Images/AndamanBasin/andaman21.jpg from DGH). Further, while correlating the shallow structures, we have also taken into account the information available from the recent International Ocean Drilling Program (IODP) Expedition-353 (Clemens et al. 2015) in the Andaman Forearc as well as IODP-362 (McNeill et al. 2016) in the Sumatra Forearc region (Fig. 2). First, various seismic horizons were digitized and their chronology was established using prior information and industry boreholes. The seismic interpretation has been carried out using Geographix$^{TM}$ software. Structural interpretations on the seismic lines are carried out within the regional stratigraphic framework.

## 3 Seismic interpretation

Based on the seismic reflection characters, lateral variations in the sedimentary geometries as well as lithological knowledge, the basin has been divided into five seismic stratigraphic units. In addition, major tectonic elements controlling the sediment depositional patterns within the basin have also been examined. Finally, the geodynamic significance of the depositional environments is discussed.

### 3.1 The Andaman Forearc Basin and its basement

The $\sim$ 900-km-long Andaman Forearc broadly extends in an N–S direction from the south of the Irrawaddy delta to the north of Sumatra, respectively, having its maximum E–W stretch of $\sim$ 50 km (Fig. 1). The Andaman Forearc exhibits a prominent gravity low between the Western Andaman Fault and the Andaman Islands with very steep gradients on either sides (Sandwell and Smith 2009; Goli and Pandey 2014). A negative gravity low of $\sim$ 70 mgal is observed along the Andaman trench followed by a broad

and distinct gravity low with an amplitude of − 100 to − 110 mgal observed over the outerarc and forearc basins. Positive gravity highs of ∼ 40–60 mgal are noted further east (Goli and Pandey 2014). The interpretation of 2D deep penetrating seismic reflection data along E–W and N–S profiles are presented in Figs. 3, 4, 5, 6 and 7. The AFB comprises of the Andaman ridge (containing the accretionary prism and the outerarc high) and a series of forearc basins towards the east (Figs. 1, 2). The seismic profiles covering the AFB and the outerarc high show that the depth to the seabed varies between ∼ 150 m (0.2 s) and ∼ 2.6 km (3.5 s in TWT) (Fig. 3). The basin shows asymmetry along its length and follows the subduction axis, with ∼ 4.5-s (TWT) thick sediments towards the north and ∼ 2.5-s (TWT) thick sediments towards the south. It also exhibits variable widths between ∼ 32 km and ∼ 50 km from north to south (Fig. 3). A prominent positive bathymetric feature between 10°N and 12°N (Figs. 1, 2) indicates the N–S asymmetric stretch of the IB. It is a > 200 km linear feature in the AFB with variable widths of < 5 km in the north and south, while > 50 km wide in the centre (Figs. 4, 6). The seismic signatures of the IB are more precisely shown in Fig. 3 with N–S extension of ∼ 175 km between SP 5200 and 12200. The sediments in the central part of the profile are upwarped uniformly (∼ 1.5 s TWT) along its entire length (Fig. 3) and are associated with a series of thrust faults. This observation corresponds to the presence of an N–S compressional regime. Roy and Chopra (1987) have reported that the IB has thick lava flows below 1100 m of middle Miocene sediments confirming its igneous nature. This significant uplift could be attributed to the upwarping of the adjoining sedimentary column of the AFB with a gradient of 1:30 (Fig. 6).

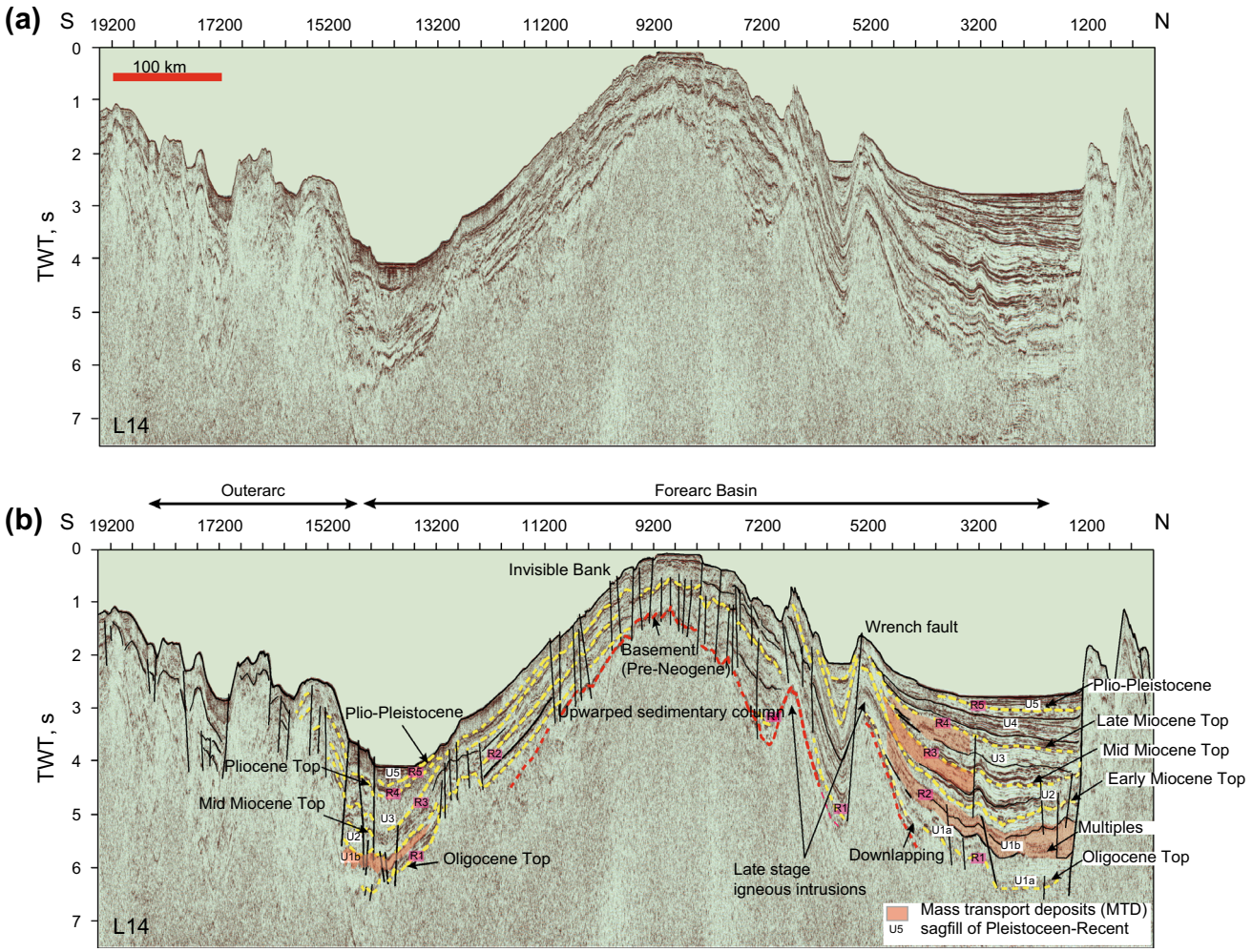


**Fig. 3** Uninterpreted (top) and interpreted seismic section through AFB along N–S seismic line L14. See Fig. 2 for location of the profile. Prominent seismic horizons R1 through R5 ranging between late Oligocene and Plio-Pleistocene between the acoustic basement and the seabed are labelled on the interpreted section. The horizontal scale bar in red represents 100 km. See text for more details

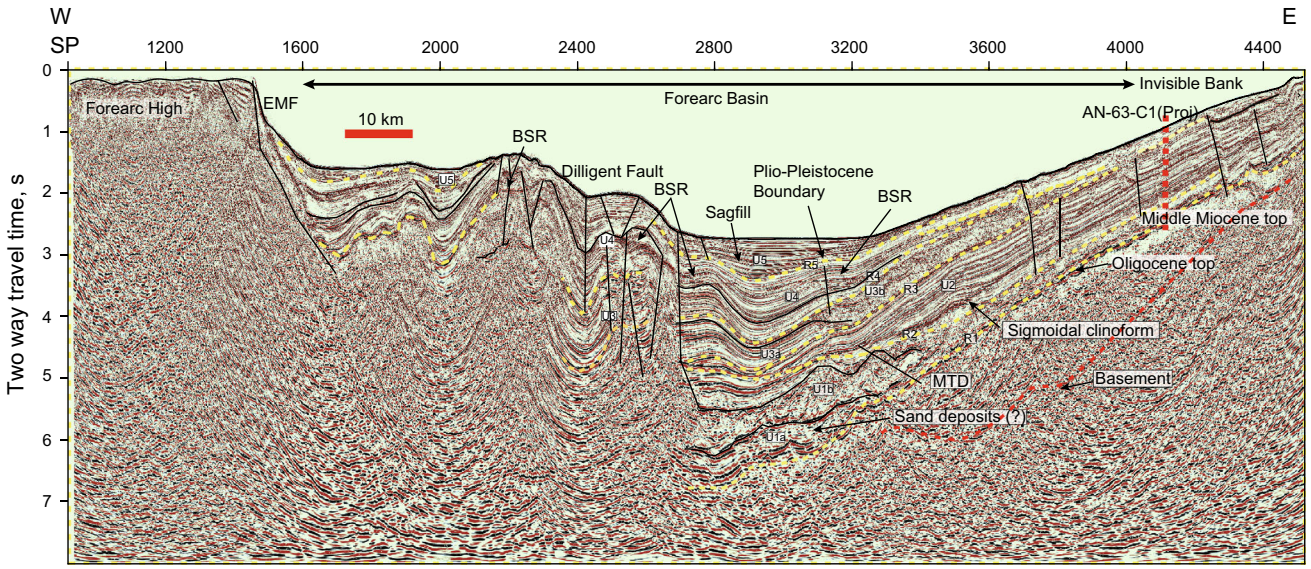


**Fig. 4** Interpreted seismic section with marked seismic horizons along E–W seismic line L5. See Fig. 2 for location of the profile. Please note the MTD deposits. The profile traverses through the entire forearc basin including forearc high, forearc basin and the Invisible Bank. The horizontal scale bar in red represents 10 km

The deepest reflector at ~ 6.5 s (TWT) is referred to as the acoustic basement in the AFB with variable dips ranging from SW–NE in the northern part to NW–SE in the southern part, respectively. The observed acoustic basement is highly deformed throughout the basin (Figs. 3, 4, 5, 6, 7). Stratigraphic interpretations from the Sumatra Forearc region (Beaudry and Moore 1985; Berglar et al. 2008; Cochran 2010; Moeremans and Singh 2015; Singh and Moeremans 2017) and recent IODP drilling results (Clemens et al. 2015; McNeill et al. 2016) show that the igneous basement underneath the southern part of the Andaman-Sumatra Forearc is overlain by the Paleogene meta-sediments. In the present study, from the northern parts of the Andaman-Sumatra Forearc, the acoustic basement is interpreted to be at ~ 6.5–7 s TWT deep. The basement in the northern part is overlain by major unconformities that are correlated with the Late Oligocene and younger times (Figs. 3, 4).

The major fault systems—East Margin Fault (EMF), Western Andaman Fault (WAF) and Diligent Fault (DF) in the AFB, are imaged on the seismic sections (Figs. 4, 6, 7). The IB—a major morphological high between the DF and WAF, is beautifully imaged on the seismic data (Figs. 4, 5, 6). Onlapping sedimentary sequences with distinct pinchouts are observed on the flanks of the IB. The total sediment thickness of various units on the eastern side is over 2 s (TWT). The basinward steeply dipping basement reflector is clearly imaged on profile L5 (Fig. 4). The WAF intersects the Andaman spreading centre ~ 10° N (Fig. 1). The spreading centre which lies slightly east of the AFB is reported to be spreading at ~ 38 mm/year (Kamesh Raju et al. 2004, 2007; Singh et al. 2013) and extends for ~ 175 km nearly perpendicular to the trench. The forearc region, to the west of the WAF, contains the mega rupture zone of the great 2004 December 26 earthquake (Gahalaut et al. 2010; Cochran 2010). The outer forearc high is separated from the Andaman ridge towards its east by EMF (Roy and Chopra 1987; Curray 2005). The EMF is marginal to the Andaman ridge containing imbricate fault structures underlain by the ophiolitic crust (Cochran 2010). The seismic profiles presented here clearly image the lateral variations of the EMF throughout the basin (Figs. 4, 5, 6). Beyond this fault, the sediments of the outerarc high/ridge are associated with severe deformation in the form of folding and faulting (Figs. 5, 6). The entire AFB including the IB is separated from the back-arc seamount complexes by the large West Andaman Fault (WAF) (Curray 2005). The seismic profiles presented here do not traverse through the seamount complex. However, on the seismic profile L1, this fault is seen as an active one (Fig. 6). Previous studies by Kamesh Raju et al. (2007) and Singh et al. (2012) have reported that WAF forms a lithospheric-scale boundary (Fig. 1). The outerarc sediments in the southern Andaman (E–W profile L1) between the shot points 2300 and 2700 are observed to be compressed giving rise to an appearance of a domal/anticline structure (Fig. 5). It suggests the influence of the Neogene deformation within the AFB region. Further east (beyond the dome structure) between SP 2900 and 3600 on the same profile, the outerarc sediments from the Neogene to Present seabed are highly folded and disrupted by thrust faulting. The troughs of these folded strata are filled with Recent sediments. These

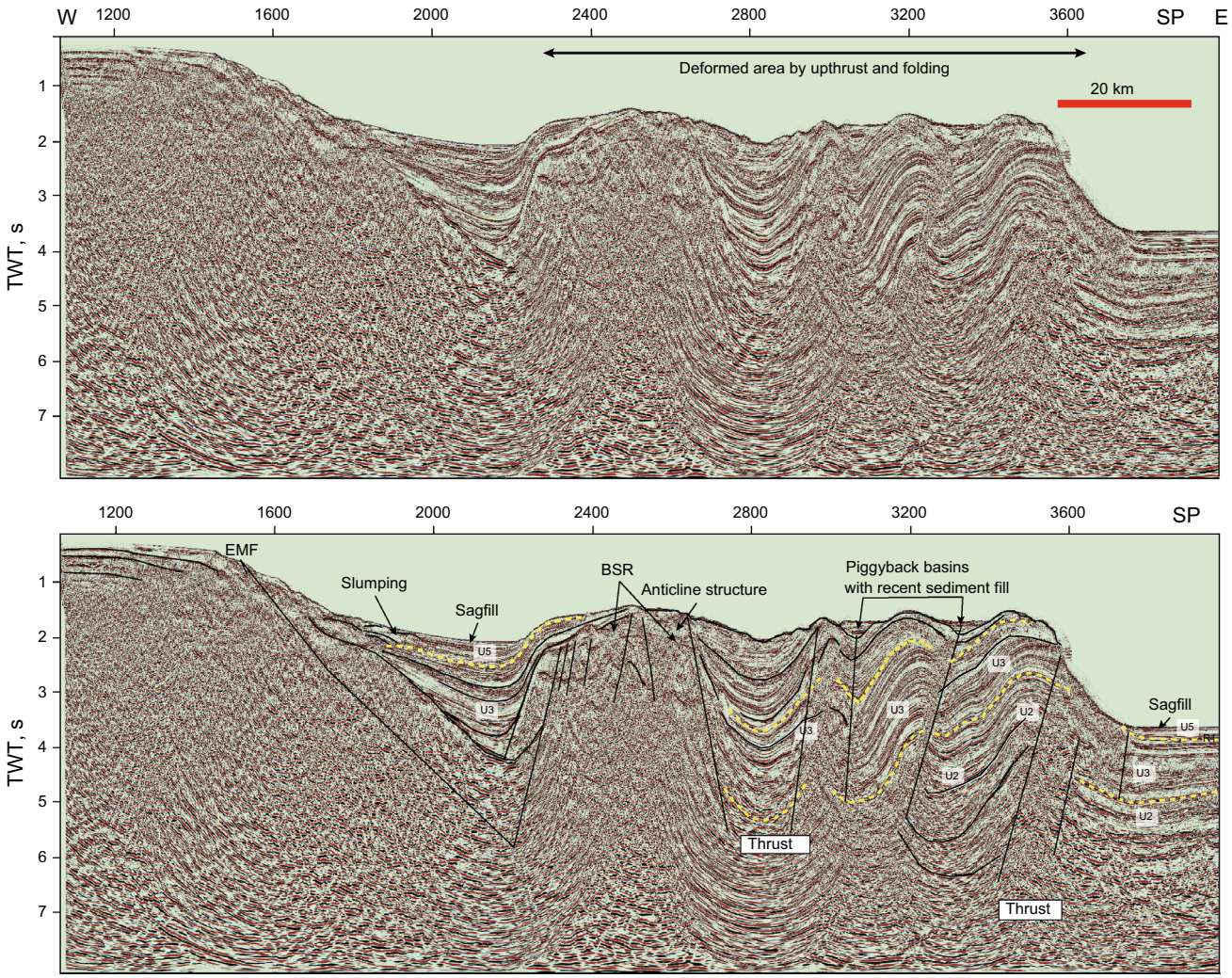


**Fig. 5** Uninterpreted (top) and interpreted seismic section along southernmost E–W seismic profile L12. See Fig. 2 for location. EMF; BSR; and other strong compressional deformations in the upper part of the crust are clearly visible on the seismic profile. The horizontal scale bar in red represents 20 km

youngest sediments occupy piggyback types of basins formed due to the consequence of thrust folds (Fig. 5). Although the source for this thrust generation is not clearly known, based on similar observations in the Sunda Forearc region (Moore et al. 1980; Harbury and Kallagher 1991; Lüschen et al. 2011), we infer that it could have originated from imbricate thrust sheets consisting of a mélange of sediments/rocks from the off-scraped sediments from the downgoing plate.

Another important observation from our interpretation is identification of bottom simulating reflectors (BSRs), a proxy indicator for gas hydrate formation (Sain and Gupta 2012; Kumar et al. 2014). We have also imaged BSRs based on their special properties on the seismic sections such as (1) mimicking the seabed with reverse polarity; (2) crosscutting the layers; and (3) overlying acoustic blanking zones. The seismic sections (Figs. 4, 5, 7) depict the presence of strong BSRs in the Early Miocene sediments of the outerarc (at crest of the dome in Fig. 7) and AFB at ~ 0.6 s (TWT) below the seabed with the water depth ranging from 0.7 to 2 km. The recent drilling activity of NGHP Expedition-01 (~ 718 m below sea floor (mbsf) has confirmed the presence of gas hydrates (~ 608 mbsf) in the volcanic ash beds of Andaman offshore (Kumar et al. 2014). The projected locations of the drilled boreholes are shown in Fig. 7.

### 3.2 Chronostratigraphy

Lithological information obtained from nearby industrial boreholes (AN-32-1, AN-27-1, AN-63-C1 and AN-1-1) (Fig. 2) by Directorate General of Hydrocarbons (DGH) has been used to establish the chronostratigraphy of the AFB (Goli and Pandey 2014). The location of NGHP

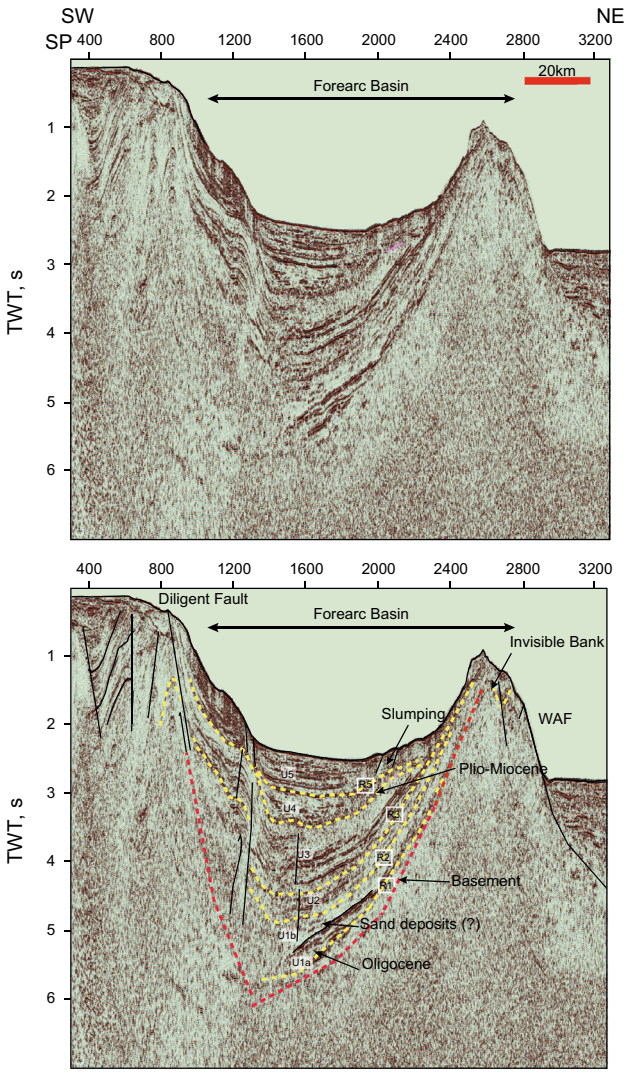


**Fig. 6** Uninterpreted (top) and interpreted seismic section (SW–NE) crossing through the Invisible Bank is shown in the figure. See Fig. 2 for location of the profile. The horizontal scale bar in red represents 20 km

Expedition-01 hole is also shown in Fig. 2. The borehole AN-1-1 was drilled to depth of ~ 3734 mbsf (Fig. 2) spanning from the Cretaceous to Recent sediments. In addition, information from two recently drilled shallow holes (U1447 and U1448) was also utilized. The two IODP sites from the IODP Expedition-353 were drilled to the depths ~ 748 and ~ 421 mbsf, respectively (Clemens et al. 2015).

Five prominent horizons have been identified based on their reflection characters and seismic terminations such as onlap and downlap, amplitude and their other properties. The acoustic basement has been mapped at a depth of ~ 6.5 s TWT which is overlain by varying sedimentary cover throughout the AFB. The deeper reflector seems to be associated with half graben-type structures both in the north and the southern sectors of the basin. This identified reflector is denoted as R1, and it corresponds to the top of the Late Oligocene (Figs. 3, 4). These major horizons/reflectors (R1 through R5) are bounded with five distinct seismic sequences (units) over the basement and have been named as U1 to U5 ranging from oldest to youngest (Figs. 3, 4). The geological ages of the key identified horizons were obtained based on correlation with the well data from the AFB (Goli and Pandey 2014) and other published information (Curray 2005; Cochran 2010; Singh and Moeremans 2017). The prominent horizons on the seismic sections represent major unconformities from the Neogene to the Recent period. As per the information available from the DGH, a total of 15 exploratory have been drilled near the Neil and Havelock Islands, of which most wells lie in the eastern Andaman offshore (www.dghindia.org). The maximum depth covered by drilling so far in the Andaman Basin is ~ 3734 m (AN-1-1) below the seabed, and the encountered sediments range from Late Cretaceous to the Recent (Fig. 2).

### 3.3 Seismic facies and stratigraphy

#### *3.3.1 Neogene base*

Horizon R1 is interpreted to be the base of the Neogene sequence in the region. This unconformity appears to be an erosional type associated with onlap deposits and is correlated with the Late Oligocene top (~ 23 Ma). The Neogene base, which is a prominent angular unconformity, is extensively traceable through most of the seismic sections (Figs. 4, 5, 6, 7). This erosional surface indicates that the depositional unit during the Early Neogene/Late Oligocene may have been subjected to subaerial exposure. It is overlain by strong, high-amplitude and continuous reflections (U1a) that appear to wedge-out at the unconformity R1. This reflector is clearly observed in the AFB especially on the northern side of the seismic profile L14 (Fig. 3). The sedimentary strata underneath R1 seem to be highly chaotic. The strata above are often cut by north and south dipping near-vertical, normal faults with variable offsets. Based on their seismic characters and coherency, it is interpreted to be most likely comprised of slumped material/sand lenses (?). The basement in this region is associated with a high degree of normal/thrust faulting that suggests considerable subsidence due to the sediment loading from terrigenous sources (Fig. 3). The remaining horizons overlying the unconformity 'R1' correspond to the tops of Early, Mid and Late Miocene to Mio-Pliocene and base of the Pleistocene boundaries, respectively (Figs. 3, 4).

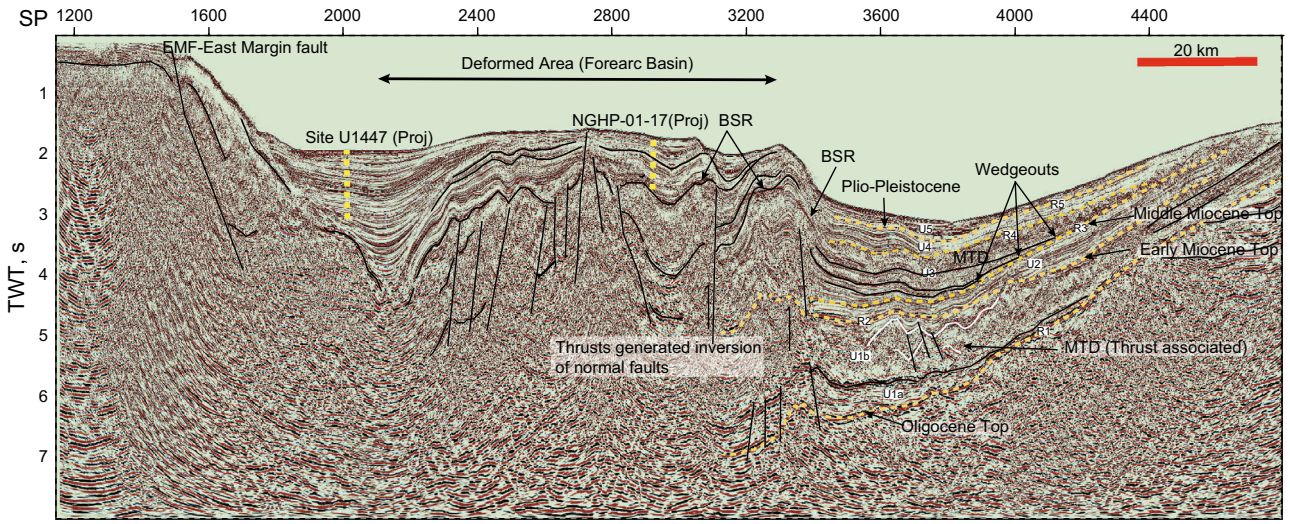


**Fig. 7** Interpreted seismic section along E–W seismic line L10. See Fig. 2 for location of the profile. Projected locations of drilling sites NGHP-01-017 and IODP site U1447 are displayed on the section. The NGHP site drilled maximum of ~ 718 m locating a BSR at ~ 608 mbsf. The total depth at site U1447 was ~ 738 mbsf

### *3.3.2 Seismic sequence U1 (Early Miocene)*

The seismic sequence U1 is bounded between R1 (reflector) and R2 as shown in Figs. 3 and 4. It consists of two distinct subunits 'U1a' and 'U1b.' Along the E–W profile, U1a shows strong concordance at boundaries, high-amplitude and parallel reflections (Fig. 4), and U1b consists of ~ 2.2-s-TWT thick unit of low amplitude, low continuity and semitransparent/hummocky reflections. The U1a shows an onlapping pattern towards the IB, which is evident in the N–S Profile as well (Fig. 3). This unit seems to be onlapping over the preexisting west dipping surface of the Oligocene top (R1). The gradual decrease in thickness of U1b towards the northern end indicates that the onlap fills would have originated from the outerarc high.

The reflection characteristics of subunits U1a and U1b appear to suggest possible sand lenses (?) and mass transport deposits (MTD), respectively (Basu et al. 2012). Both the weak reflectivity and the low seismic coherency of the lower seismic facies support interpretation as slump material. On the other hand, the high-amplitude reflections of the overlying unit suggest an alternation of turbidite/pelagic nature. The internal reflections within the unit U1b occasionally exhibit small-scale folding. The internal architecture and chaotic facies within the MTDs suggest possibility of syn-depositional thrusts that could also be linked to the imbricate geometry of the region.

### *3.3.3 Seismic sequence U2 (Mid-Miocene)*

Seismic sequence 'U2' consists of a convergent sedimentary package that gradually thins from 1 to 0.1 s TWT as shown in Fig. 4 (SP 4500 and 2900). The internal reflections within this sequence are 'S'-shaped (sigmoidal) with medium amplitude and high continuity. The lower boundary (R2) of this sequence is associated with basinward shift of the downlapping reflections of 'U2' sediments. The sloping depositional surface with sigmoidal progradation into deepwater is defined as clinoform (Mitchum et al. 1977). The clinoforms indicate sedimentation during synchronous Mid-Miocene to Early Pliocene regressive phases (see Table 1). Intermittent tectonic activities during the Mid-Miocene to the Early Pliocene regressive cycle appear to be accompanied with sporadic intrusions and volcanism. This Neogene phase is also regarded as one of the peak regressive phases in Southeast Asia (Haq et al. 1987). Figure 4 shows the E–W profile that crosses the IB where a sigmoidal clinoform is seen prominently towards the eastern margin of the AFB. This supports our contention that the key role behind the Neogene sedimentation process in the region is played by regional tectonics (uplift of the IB). In contrast, absence of such clinoforms in other E–W profiles (Fig. 6) provides an important clues about impact of past tectonic activities along N–S extent of the IB.

### *3.3.4 Seismic sequence U3 (Late Miocene) and seismic sequence U4 (Pliocene)*

The Mid-Miocene top (R3) is overlain by unit U3, which is further divided into two subunits, namely U3a and U3b. Unit U3a is a wedge-shaped toplapping unit exhibiting strong continuity and moderate amplitude reflections, representing a progradational environment (Fig. 4 and Table 1). Beyond the SP 3200 towards the east, the continuity of U3a is not very clear. U3b (between SP 2900 and

**Table 1** Description of seismic facies analyses used for identification of various units on the seismic sections

| Comments | Depositional environment | Reflection Geometry: Reflection configuration | Reflection Geometry: Reflection amplitude | Reflection Geometry: Reflection continuty | Seismic units/ Sequences | Epoch | | Sea lecel (High 100 — Low 0 m) / Age (in My) |
|---|---|---|---|---|---|---|---|---|
| Normal deposition with no or less tectonic effet | Sagfill | Parallel | Moderate to high | Continuous | U5 | Quaternary | | |
| | | | | | R5 | | | |
| Basin fill under tectonics effect | Basin fill | Wavy | Low to moderate | Continuous | U4 | Pliocene | L | |
| | | | | | | | E | |
| | | | | | R4 | | | |
| MTD | Progradational | Chaotic | Low | Discontinuous (U3b) | U3 (U3b, U3a) | | L | |
| MTD | Basin fill | Wavy | Low to moderate | Continuous (U3a) | | | | |
| | | | | | R3 | Miocene | | |
| MTD (due to uplift of Invisible bank) | Sigmoidal progradation | S-shaped | Moderate to high | Continuous | U2 | | M | |
| | | | | | R2 | | | |
| MTD | Onlap fill | Semitrasparent/Chaotic & moderately wavy | Low | Discontinuous (U1b) | U1 (U1b, U1a) | | E | |
| Sand deposits (?) | Onlap fill | Moderately wavy | High | Moderately Continuous (U1a) | | | | |
| | | | | | Neogene Base (R1) | | | |
| | | | | | | Oligocene | | |

(Haq et al., 1987)

The right panel shows sea level curve of Haq et al. (1987)

3300) is immediately underlain by U3a, which exhibits progradational characteristics (onlap at the top and downlap at the base) of sediments (Fig. 4). According to Haq et al. (1987), relative fall in the global sea level has been reported during the Early Miocene which can broadly be attributed to the sediment progradation seen in U3b. However, it must be noted that the global sea level fluctuations represent a combination of factors such as eustasy, subsidence and sediment supply. This unit (U3b) consists of a semitransparent, chaotic reflection pattern suggesting mass transport deposition (MTD). The depocenter of U3a is shifted to the outerarc, whereas U2 seems to be placed towards IB in the East. Such fluctuating depocenters suggest that varied sources (IB in East and outerarc high in the west) were responsible for the depositional environment in the AFB.

It is difficult to differentiate between overlying seismic sequence 'U4' (Pliocene sediments) from seismic sequence 'U3' (Late Miocene sediments) because of their high similarity in reflection characters like strong lateral continuity, medium amplitude and slightly folded reflections. Based on their reflection characteristics, we interpret that these deposits are related to turbidity fills, which were perhaps controlled by increased volcanic activity and outgrowth of the outerarc during the Late Miocene (U3) and the Pliocene (U4), respectively (Karig et al. 1979; Moore and Karig 1980; Seeber et al. 2007; Mosher et al. 2008).

### *3.3.5 Seismic sequence U5 (Pleistocene to Recent)*

Seismic sequence U5 is bounded by the overlying seabed and the prominent reflector R5 (Plio/Pleistocene boundary). This unit, which consists of parallel and continuous reflections with medium to high amplitude, settled over the reflector R5 with sag-like geometry (Figs. 3, 4, 5, 6, 7). The updip reflection pattern of these sag fill deposits towards the east permits the inference that U5 was tectonically disturbed by uplift processes, similar to that seen in the Mio-Pliocene beds. Therefore, it can be suggested that anticline growth towards the east occurred during the Pliocene and was subsequently overlain by sediments pertaining to the U5 sequence.

The occurrence of slump-related structures as observed in the Middle Andaman region (Fig. 6), to the east of the AFB, indicates that slope failures must have occurred due to the high gradient. Such events could most likely be explained by Pleistocene to Recent uplift/tectonic activities around the IB. The chaotic and semitransparent nature of reflection patterns (Stoker et al. 1991) seen in the upper part of U5 agrees with the presence of westward dipping slumping structures.

## 4 Discussion

The latest plate tectonic reconstruction models (Hall 1996, 2011, 2012; Gibbons et al. 2015 and references therein) suggest that between 90 and 75 Ma, India and Australia were separated by a leaky transform boundary. From 85 Ma, the Indian plate moved rapidly northward finally resulting in the subduction at the India-Eurasia margin (Liu et al. 1983; Daly et al. 1991; Hall 1996, 2012). Plate motion evolved more dynamically as converging from ~ 75 to ~ 55 Ma. Initially, the collision of the Indian plate with SE Asia occurred with a high convergence rate of about 100 mm/year (Curray 2005 and references therein). During the Middle Eocene, the convergence rate slowed to 60 mm/year (Lee and Lawver 1995), which led to the development of many extensional basins in the region (Curray 2005; Decelles et al. 2011; Hall 2012; Singh et al. 2013). The process of subduction was initiated at around 45 Ma near the Java trench. A widespread spreading in the Indian Ocean during the Late Eocene–Early Oligocene led to: (i) a change in convergence direction from north to NE and (ii) an increase in the rate of subduction (50–60 mm/year) along the Andaman-Sumatra and Java margins (Karig et al. 1979; Liu et al. 1983; Daly et al. 1991; Hall 2012; Gibbons et al. 2015). This spreading also in turn initiated the development of the Neogene AFB along the Sunda trench to the Andaman arc. The hard collision of the Indian and Eurasian plates (Curray 2005; Decelles et al. 2011) in the Late Oligocene to the Early Miocene time is the cause of huge deposition of terrigenous sediments into the Indian Ocean and the trench region. Our seismic interpretations support consistently slow and steady sedimentation during the Late Oligocene to the Early Miocene (Figs. 4, 5, 6, 7). The sediments that were scraped off subsequently gave rise to the large accretionary wedge (Matson and Moore 1992; Cochran 2010; Singh et al. 2013) followed by the development of the Neogene AFBs.

The oblique subduction along Andaman-Sumatra is the cause for partition of strain into an orthogonal component which resulted in thrust faulting in the Andaman-Nicobar ridge and right lateral strike-slip faulting (Katili 1973; Hamilton 1979, 1988; Moore et al. 1980; McCaffrey 1992; McCaffrey et al. 2000; Malod et al. 1995; Pal et al. 2002, 2003; Moeremans and Singh 2015). Seismic images from the AFB presented here confirm Late Miocene and onwards rapid growth of the forearc region. The Paleogene sequences overlying the acoustic basement in the AFB (Figs. 4, 7) depict strong erosional unconformities and are attributed to the Late Oligocene regressive cycles.

Based on seismic reflection patterns, 4.5-s (TWT) thick sediments which settled over the Neogene base (R1) are divided into five different seismic sequences (U1–U5) for the present study. Depositional ages have been inferred based on correlation of sequence boundaries from the well data and seismic unconformities. It is evident from the interpretation that the AFB is filled with the Neogene to Recent sediments with five distinct sequences (Figs. 3, 4, 5, 6, 7). These sequences correspond to the Pleistocene and younger sag fill sediments, underlain by tectonically affected older (Neogene) basin-fill sediments.

A strong reflector at ~ 6.5 s TWT (the Neogene base) is immediately overlain by U1, which corresponds to Early Miocene sediments and consists of two subunits U1a and U1b—(i) onlapping unit (U1a) of strong and high-amplitude reflections and (ii) a unit (U1b) of hummocky and semitransparent reflections and bounded with less deformed (folded) strata as the upper boundary (Fig. 4), indicating the probable presence of sand deposits (turbidity) and MTDs (debris). Along the N–S profile, U1a is associated with a downlap unit showing divergent reflection patterns (towards IB), indicating a deposition from syn-tectonics subsidence. These subunits within the Early Miocene overlying the basement indicate that these depositional units in many parts of the AFB were subjected to the subsequent uplift of the basement on the eastern rim.

Towards Southern Andaman (Fig. 1), most of the E–W profiles, which traverse across or nearer to the top of the IB, show progradational deposits between the Early and Mid-Miocene (Fig. 4). From the eustatic sea level curve (Table 1), it appears that the magnitude of fluctuations is not very high during this time. Therefore, it may be highly likely that these changes could have been caused by regional tectonics, rather than sea level fluctuations. The major unconformity referred by R3 corresponds to the Mid-Miocene top, overlain by turbidity flows with a small pack of continuous reflections (U3a) mostly wedging out at the preexisting surface of R3. This unit underlies a unit (U3b) of MTD with semitransparent and hummocky reflections. From the Late Miocene to the Plio-Pleistocene stratification within the basin is more or less uniform and consists of continuous reflections with medium amplitude and onlap towards the prominent unconformity (R3) below. During the Late Pliocene, the huge sediment supply was caused by a cumulative effect of sea level fall in the Late Miocene and increased transgression activity in the Pliocene (Pal et al. 2002, 2003; Susilohadi et al. 2005). Along with this sediment supply, a rapid outgrowth of the outerarc ridge towards the west of the basin (during the Pliocene) caused subsidence. Towards the southern sector of the study area, the AFB sediments of the Oligocene to Plio-Pleistocene were upwarped and squeezed into the form of a buried domal (anticline) structure (Figs. 4, 5). The depression (basin) which spreads between the Andaman-Nicobar ridge bounded by a right lateral strike-slip fault (i.e., EMF) and

IB has been separated into two linear basin elements by this anticlinal structure (Fig. 5).

Along the E–W seismic profile (Fig. 5), the onlapping seismic unit (U5) of Pleistocene to Recent sediments occurring over the preformed flexure structure helps in inferring that this event of up-thrusting has taken place during Pleistocene–Recent time towards the northern forearc, but in the northern sector, the presence of this dome-like feature is not very clear (Fig. 3). Towards the south, the formation of these domal/folded features with thrust faults spread over a length of ~ 27 km along E–W direction (Figs. 5, 7) indicates a zone of recent compressional uplift with probable linkage to the regional tectonics. These deformed sediments of the trough fill beyond EMF are separated from the AFB by a major thrust fault further east (Figs. 4, 5, 6, 7). The entire western rim of the AFB from north to south is associated with the domal-shaped seabed topography caused by the late Oligocene to Miocene upthrust activities. The uplifted part is separated from the surrounding basin configuration by an old marginal fault (of most likely pre-Miocene time). It also seems to have been reactivated in Recent times as evident from the updip reflection of sag fill deposition towards the basin (Figs. 4, 5, 6, 7). Along E–W profile L4, the acoustic basement (the Oligocene top) between SP 3100 and 3300 is inferred as a westward dipping surface, deformed by normal faults (Fig. 7) and overlain by an upthrust sedimentary column of the Mid-Miocene–Recent age. The seismic reflection pattern within this entire assemblage suggests significant reactivation of small-scale faults prior to the Early Miocene that may have caused substantial deformation within the strata (Fig. 7). The seismic images along this line further show that the upthrusts partly extend towards the interior of the basin. Regional reactivation of faults during the same time has also been reported in the Sumatra Forearc region by Berglar et al. (2008).

Based on the seismic interpretation shown here, it appears that the uplift of the IB was an episodic phenomenon. Preliminary uplift may have taken place in the Early Oligocene and then again in the Mid-Miocene followed by the Pleistocene to Recent. This episodic uplift of the IB towards the east and reactivated faults (Recent upthrust) towards west may be collectively responsible for further subsidence of the basin.

The Pleistocene to Recent sediments are generally mostly characterized by laterally continuous reflections and can be clearly distinguished from the underlying Pliocene sediments displaying a regressive surface (R6) as shown in Fig. 3. The gradient and relief of this uplifted bank varies in the N–S profile as shown in Fig. 3. In the middle Andaman, U5 contains Recent sediment deposition, which is partly associated with westward dipping slumping structures (Fig. 6). Slumps are identified by the chaotic and semitransparent nature of the reflection pattern (Stoker et al. 1991). These slumps were transported eastward, indicating that the slope failures formed by high slope gradient may be interlinked to the uplift of the IB.

## 5 Conclusion

The present study focuses on the seismic reflection imaging of the AFB including the outerarc high and IB towards the east. The water depth in the study area varies from ~ 0.15 km to ~ 2.6 km. From our stratigraphic interpretation of the new regional seismic lines, it is inferred that the AFB is filled with ~ 4.5-s-TWT thick Neogene to Recent sediments with two distinct broad sequences of Neogene (U1–U4) and Quaternary (U5). The Neogene sediments were mostly driven by repeated tectonism, whereas basin-fill deposits were caused by various episodes of mass transport (Table 1) both from outerarc and IB. On the other hand, Quaternary sediments primarily consist of sag fill deposits in the AFB. Our interpretation has brought out a stratigraphic framework within the AFB, which compliments similar studies (e.g., Ghosal et al. 2012; Singh et al. 2013; Moeremans and Singh 2015) published from the southern segment of the Andaman-Sumatra subduction system. The accretionary prism in the region contains several weak zones that could be potential rupture targets in the event of large earthquakes. The AFB contains compressional regimes much similar to that in the southern part of this subduction system. The EMF is a marginal normal fault with easterly dips, whereas the DF comprises of a collective thrust faulted units adjoining IB. The uplift of the IB appears to have occurred episodically, which agrees with previous studies (Curray 2005; Singh and Moeremans 2017). We infer that it may have undergone a preliminary uplift in the Early Oligocene time followed by deformational activities since the Mid-Miocene. The inferred wrench fault at IB suggests a late stage deformation, which in turn could have been the cause for erosion of uplifted younger sediments. The western rim of the basin is mainly associated with reactivation of half grabens (normal faults) on top of the Early Miocene sediments. Both margins of the basin are associated with tectonic uplift of varied intensities and are most likely the cause for slope failure deposits. The documented slope failures within the youngest strata having westward dips further suggest active deformation of IB. The presence of strong BSR at a depth of 0.6 s below the seabed in the Miocene sediments of the outerarc and AFB suggest occurrence of gas hydrates in the Andaman offshore region in contrast to the Sunda subduction zone. The new seismic images of complete depositional units from the AFB are presented above. Our new results discussed here have potential implications for the

tectono-sedimentary evolution of this region. In view of the limited penetration (~ 7 s TWT), more precise details may emerge from a deep penetrating seismic survey in the near future.

**Acknowledgements** We thank Director, National Centre for Antarctic and Ocean Research, Goa, for permission to submit this manuscript. We are also thankful to Directorate General of Hydrocarbons (DGH) for providing the multichannel seismic (MCS) reflection data. This is NCAOR Contribution No. 10/2017.



## References

Basu P, Verma R, Paul R, et al. Mass-transport complexes in deep water of Andaman Forearc Basin. Geohorizons. 2012;1:46–9.

Beaudry D, Moore GF. Seismic stratigraphy and Cenozoic evolution of West Sumatra Forearc basin. AAPG Bull. 1985;69(5):742–59.

Berglar K, Gaedicke C, Lutz R, et al. Neogene subsidence and stratigraphy of the Simeulue Forearc basin, Northwest Sumatra. Mar Geol. 2008;253(1–2):1–13. doi:10.1016/j.margeo.2008.04.006.

Berglar K, Gaedicke C, Franke D, et al. Structural evolution and strike-slip tectonics off north-western Sumatra. Tectonophysics. 2010;480(1–4):119–32. doi:10.1016/j.tecto.2009.10.003.

Clemens SC, Kuhnt W, LeVay LJ, and the Expedition 353 Scientists. Indian monsoon rainfall. International Ocean Discovery Program Preliminary Report 353. 2015. doi:10.14379/iodp.pr.353.2015.

Cochran JR. Morphology and tectonics of the Andaman Forearc, northeastern Indian Ocean. Geophys J Int. 2010;182(2):631–51. doi:10.1111/j.1365-246X.2010.04663.x.

Curray JR. Tectonics and history of Andaman sea region. Asian Earth Sci. 2005;25:187–232. doi:10.1016/j.jseaes.2004.09.001.

Curray JR, Moore DG, Lawve LA, et al. Tectonics of the Andaman Sea and Burma. In: Watkins, JS, Montadert L, Dickerson PW, editors. Geological and geophysical investigations of continental slopes and rises. vol. 29. AAPG Memoir; 1979. p. 189–98.

Daly MC, Cooper M, Wilson I, et al. Cenozoic plate tectonics and basin evolution in Indonesia. Mar Pet Geol. 1991;8(1):2–21.

DeCelles PG, Kapp P, Quade J, et al. Oligocene–Miocene Kailas basin, southwestern Tibet: record of postcollisional upper-plate extension in the Indus-Yarlung suture zone. GSA Bull. 2011;123(7–8):1337–62. doi:10.1130/B30258.1.

Gahalaut VK, Subrahmanyam C, Kundu B, et al. Slow rupture in Andaman during 2004 Sumatra–Andaman earthquake: a probable consequence of subduction of 90 E ridge. Geophys J Int. 2010;180(3):1181–6. doi:10.1111/j.1365-246X.2009.04449.x.

Ghosal D, Singh SC, Chauhan A, et al. New insights on the Great Sumatran Fault, NW Sumatra, from marine geophysical studies. Geochem Geophys Geosyst. 2012. doi:10.1029/2012GC004122.

Gibbons AD, Zahirovic S, Müller RD, et al. A tectonic model reconciling evidence for the collisions between India, Eurasia and intra-oceanic arcs of the central-eastern Tethys. Gondwana Res. 2015;28(2):451–92. doi:10.1016/j.gr.2015.01.001.

Goli A, Pandey DK. Structural characteristics of the Andaman Forearc inferred from interpretation of multichannel seismic reflection data. Acta Geol Sin Engl. 2014;88(4):1145–56. doi:10.1111/1755-6724.12279.

Hall R. Reconstructing Cenozoic SE Asian terranes. In: Hall R, Blundell D, editors. Tectonic evolution of Southeast Asia. vol. 106. Geol Soc London Spec Pub; 1996. p. 153–84.

Hall R. Australia–SE Asia collision: plate tectonics and crustal flow. Geol Soc London. 2011;355:75–109. doi:10.1144/SP355.5.

Hall R. Late Jurassic-Cenozoic reconstructions of the Indonesian region and the Indian Ocean. Tectonophysics. 2012;570:1–41. doi:10.1016/j.tecto.2012.04.021.

Hamilton W. Tectonics of the Indonesian region. Geological Survey Professional Paper 1078: 1 plate. Washington, DC: US Government Printing Office; 1979. p. 345.

Hamilton W. Plate tectonics and island arcs. GSA Bull. 1988;100(10):1503–27. doi:10.1130/0016-7606(1988)100<1503:PTAIA>2.3.CO;2.

Haq BU, Hardenbol J, Vail P. Chronology of fluctuating sea levels since the Triassic. Science. 1987;235(4793):1156–67. doi:10.1126/science.235.4793.1156.

Harbury NA, Kallagher HJ. The Sunda outer-arc ridge, North Sumatra, Indonesia. J SE Asian Earth Sci. 1991;6(3–4):463–76. doi:10.1016/0743-9547(91)90088-F.

Izart A, Kemal BM, Malod JA. Seismic stratigraphy and subsidence evolution of the northwest Sumatra fore-arc basin. Mar Geol. 1994;122(1–2):109–24. doi:10.1016/0025-3227(94)90207-0.

Kamesh Raju KA, Ramprasad T, Rao PS, et al. New insights into the tectonic evolution of the Andaman Basin, northeast Indian Ocean. Earth Planet ScI Lett. 2004;221(1–4):145–62. doi:10.1016/S0012-821X(04)00075-5.

Kamesh Raju KA, Murty GPS, Amarnath D, et al. The West Andaman Fault and its influence on the aftershock pattern of the recent megathrust earthquakes in the Andaman–Sumatra region. Geophys Res Lett. 2007. doi:10.1029/2006GL028730.

Karig DE, Suparka S, Moore GF, et al. Structure and Cenozoic evolution of the Sunda Arc in the central Sumatra region. In: Watkins JS, Montadert L, Dickerson PW, editors. Geological and geophysical investigations of continental margin. vol. 29. AAPG Memoir; 1979. p. 189–98.

Katili JA. Geochronology of west Indonesia and its implication on plate tectonics. Tectonophysics. 1973;19(3):195–212. doi:10.1016/0040-1951(73)90019-X.

Katili JA. Volcanism and plate tectonics in the Indonesian-island arcs. Tectonophysics. 1975;26(3–4):165–88. doi:10.1016/0040-1951(75)90088-8.

Kumar P, Collett TS, Boswell R, et al. Geologic implications of gas hydrates in the offshore of India: Krishna-Godavari Basin, Mahanadi Basin, Andaman Sea, Kerala-Konkan Basin. Mar Pet Geol. 2014;58:29–98. doi:10.1016/j.marpetgeo.2014.07.031.

Lee TY, Lawver LA. Cenozoic plate reconstruction of Southeast Asia. Tectonophysics. 1995;251(1–4):85–138. doi:10.1016/0040-1951(95)00023-2.

Liu CS, Curray JR, McDonald JM. New constraints on the tectonic evolution of the eastern Indian Ocean. Earth Planet Sci Lett. 1983;65(2):331–42. doi:10.1016/0012-821X(83)90171-1.

Lüschen E, Müller C, Kopp H, et al. Structure, evolution and tectonic activity of the eastern Sunda forearc, Indonesia, from marine seismic investigations. Tectonophysics. 2011;508(1):6–21. doi:10.1016/j.tecto.2010.06.008.

Malod JA, Karta K, Beslier MO, et al. From normal to oblique subduction: tectonic relationships between Java and Sumatra. J SE Asian Earth Sci. 1995;12(1–2):85–93. doi:10.1016/0743-9547(95)00023-2.

Matson R, Moore GF. Structural controls on Forearc basin subsidence in the central Sumatra Forearc basin. Geol Geophys Cont Margins AAPG Mem. 1992;53:157–81.

McCaffrey R. Oblique plate convergence, slip vectors, and forearc deformation. J Geophys Res. 1992;97(B6):8905–15. doi:10.1029/92JB00483.

McCaffrey R. The tectonic framework of the Sumatra subduction zone. Annu Rev Earth Planet Sci. 2009;37:345–66. doi:10.1146/annurev.earth.031208.100212.

McCaffrey R, Zwick PC, Bock Y, et al. Strain partitioning during oblique plate convergence in northern Sumatra: geodetic and seismologic constraints and numerical modeling. J Geophys Res. 2000;105(B12):28363–76. doi:10.1029/1999JB900362.

McNeill L, Dugan B, Petronotis K. Expedition 362 Scientific Prospectus: the Sumatra subduction zone. Int Ocean Discov Prog. 2016. doi:10.14379/iodp.sp.362.2016.

Mitchum Jr RM, Vail PR, Sangree JB. Seismic stratigraphy and global sea level, Part 6: stratigraphy interpretation of seismic reflection pattern in depositional sequences. In: Payton CE, editor. Seismic stratigraphy-applications to hydrocarbon exploration. vol. 26. AAPG Bull; 1977. p. 117–33.

Moeremans R, Singh SC. Fore-arc basin deformation in the Andaman-Nicobar segment of the Sumatra-Andaman subduction zone: insight from high-resolution seismic reflection data. Tectonics. 2015;34(8):1736–50. doi:10.1002/2015TC003901.

Moeremans R, Singh SC, McArdle J, et al. Seismic images of structural variations along the deformation front of the Andaman-Sumatra subduction zone: implications for rupture propagation and tsunamigenesis. Earth Planet Sci Lett. 2014;386:75–85. doi:10.1016/j.epsl.2013.11.003.

Moore GF, Karig DE. Structural geology of Nias Island, Indonesia: implication for subduction zone tectonics. Am J Sci. 1980;280(3):193–223. doi:10.2475/ajs.280.3.193.

Moore GF, Curray JR, Moore DG, et al. Variations in deformation along the Sunda Forearc, northeast Indian Ocean. In: Hayes DE, editor. AGU Geophys Monograph. vol. 23; 1980. p. 45–160.

Mosher DC, Austin JA, Fisher D, et al. Deformation of the northern Sumatra accretionary prism from high-resolution seismic reflection profiles and ROV observations. Mar Geol. 2008;252(3–4):89–99. doi:10.1016/j.margeo.2008.03.014.

Pal T, Gupta TD, Das Gupta SC. Vitric tuff from Archipelago Group of rocks (Mio-Pliocene) of south Andaman. J Geol Soc India. 2002;59(2):111–4.

Pal T, Chakraborty PP, Gupta TD, et al. Geodynamic evolution of the outer-arc–forearc belt in the Andaman Islands, the central part of the Burma-Java subduction complex. Geol Mag. 2003;140(3):289–307. doi:10.1017/S0016756803007805.

Peltzer G, Tapponnier P. Formation and evolution of strike-slip faults, rifts and basins during the India-Asia collision: an experimental approach. J Geophys Res. 1988;93(B12):15085–117. doi:10.1029/JB093iB12p15085.

Rao NP, Kumar MR. Evidence for cessation of Indian plate subduction in the Burmese arc region. Geophys Res Lett. 1999;26(20):3149–52. doi:10.1029/1999GL005396.

Rodolfo KS. Bathymetry and marine geology of the Andaman basin and tectonic implications for Southeast Asia. Geol Soc Am Bull. 1969;80(7):1203–30. doi:10.1130/0016-7606(1969)80[1203:BAMGOT]2.0.CO;2.

Roy TK, Chopra, NN. Wrench faulting in Andaman Forearc basin, India. In: Proceedings Offshore Technology Conference. vol. 19; 1987. p. 393–404. doi:10.4043/5465-MS.

Sain K, Gupta H. Gas hydrates in India: potential and development. Gondwana Res. 2012;22(2):645–57. doi:10.1016/j.gr.2012.01.007.

Sandwell DT. Smith W.H.F. Global marine gravity from retracked Geosat and ERS 1 altimetry: ridge segmentation v. spreading rate. J Geophys Res. 2009;114:B01411. doi:10.1029/2008JB006008.

Seeber L, Mueller C, Fujiwara T, et al. Accretion, mass wasting, and partitioned strain over the Dec 2004 Mw9.2 rupture offshore Aceh, northern Sumatra. Earth Planet Sci Lett. 2007;263(1–2):16–31. doi:10.1016/j.epsl.2007.07.057.

Sieh K, Natawidjaja D. Neotectonics of the Sumatran fault, Indonesia. J Geophys Res. 2000;105(B12):28295–326. doi:10.1029/2000JB900120.

Singh SC, Moeremans R. Anatomy of the Andaman Nicobar Subduction System from seismic reflection data. Geol Soc Lond Mem. 2017;47:193–204. doi:10.1144/M47.13.

Singh SC, Chauhan APS, Calvert AJ, et al. Seismic evidence of bending and unbending of the subducting oceanic crust and the presence mantle megathrust in the 2004 earthquake rupture zone. Earth Planet Sci Lett. 2012;321–322:166–76. doi:10.1016/j.epsl.2012.01.012.

Singh SC, Moeremans R, McArdle J, et al. Seismic images of the sliver strike-slip fault and backthrust in the Andaman-Nicobar region. J Geophys Res. 2013;118(10):5208–24. doi:10.1002/jgrb.50378.

Stoker MS, Harland R, Graham DK. Glacially influenced plain sedimentation in the southern Faeroe-Shetland channel, northwest United Kingdom continental margin. Mar Geol. 1991;100(1–4):185–99. doi:10.1016/0025-3227(91)90232-S.

Susilohadi S, Gaedicke C, Ehrhardt A. Neogene structures and sedimentation history along the Sunda Forearc basins off southwest Sumatra and southwest Java. Mar Geol. 2005;219(2–3):133–54. doi:10.1016/j.margeo.2005.05.001.